

RESEARCH

Open Access



Joint interference alignment and power allocation for NOMA-based multi-user MIMO systems

Mohamed Rihan^{1,2}, Lei Huang¹ and Peichang Zhang^{1*}

Abstract

Interference alignment (IA) and non-orthogonal multiple access (NOMA) are key technologies for achieving the capacity scaling required by next generation networks to overcome the unprecedented growth of data network traffic. Each of these technologies was proved to present excellent performance for MIMO systems. In this article, we propose a joint IA and power allocation (PA) framework for NOMA-based multi-user MIMO (MU-MIMO) systems. Different approaches for applying IA in downlink NOMA-based MU-MIMO systems will be addressed while implementing a PA technique that fully exploits the characteristics of NOMA-based systems. The proposed framework aims to maximize the sum-rate of the NOMA-based MU-MIMO system through combining IA with PA. The process begins by initially grouping the system users into clusters for optimum implementation of NOMA. The sum-rate maximization is carried out under cluster power budget, user quality-of-service (QoS), and robust successive interference cancellation (SIC) constraints. Meanwhile, it uses the power domain multiplexing strategy to allow the users within each cluster to share the data streams without exerting interference to one another. Three iterative joint IA and PA algorithms are proposed for NOMA-based MU-MIMO systems. Moreover, these algorithms are compared with orthogonal multiple access (OMA)-based MU-MIMO counterpart as well as the state-of-the-art techniques presented for NOMA-based MU-MIMO systems. Numerical simulations verify that the proposed framework can greatly improve the performance of NOMA-based MU-MIMO systems in terms of the achievable sum-rate when compared with OMA-based MU-MIMO and the state-of-the-art NOMA-based MU-MIMO systems.

Keywords: Non-orthogonal multiple access (NOMA), Interference alignment (IA), Power allocation, Joint optimization, Grassmann manifold

1 Introduction

One of the key challenges facing the fifth generation (5G) mobile networks is the overwhelming growth of data network traffic. Accordingly, non-orthogonal multiple access (NOMA) has recently attracted much attention as a promising radio access technology in 5G mobile networks due to its superior spectral efficiency [1]. The concept behind NOMA is the exploitation of the power domain for implementing a multiple access mechanism in mobile networks. Specifically, the signals of NOMA users are assigned with different power

allocation (PA) coefficients according to their channel conditions. Users with poor channel conditions are assigned more power level, and users with better channel conditions are assigned lower power level [2, 3]. One of the major advantages of the NOMA technique is its excellent ability to balance between sum-rate and fairness, and accordingly achieves an optimized spectral efficiency for all the served users [2, 4].

The NOMA technique was the core of many research studies in the last few years [1–7]. In [5], a comparison between NOMA and its orthogonal counterparts, in terms of the achievable sum-rate, has been accomplished and the results demonstrated the superiority of NOMA as a radio access technology for future 5G cellular networks. In [6], the NOMA technique is used to implement a cooperative transmission strategy for spectrum-sharing

*Correspondence: pzhang@szu.edu.cn

¹Multi-dimensional Signal Processing Lab., College of Information Engineering, Shenzhen University, Shenzhen, China

Full list of author information is available at the end of the article

cognitive radio networks. The user fairness for NOMA-based cellular systems has been addressed in [4]. NOMA technique is also used in cognitive radio networks in order to maintain some pre-defined quality-of-service (QoS) conditions [7]. The application of MIMO-NOMA to the downlink mobile communication networks is addressed in [2]. Specifically, they implement MIMO-NOMA to both cellular and cognitive inspired wireless networks. Additionally, they explored the outage probability for MIMO-NOMA systems and study the sum-rate gap between NOMA-based networks and their orthogonal multiple access (OMA) counterparts.

During the last decade, interference alignment (IA) technique is also proposed as an excellent solution to the interference problem arising in wireless multi-user (MU) communication networks that significantly improve its sum-rate [8]. Specifically, implementing IA technique in wireless networks results in sum-rate that can scale linearly and without bound with the number of users in the network at high signal-to-noise power ratio (SNR) [8, 9]. The key idea behind the IA technique is to align interference signals into a reduced dimensional subspace leaving the remaining subspace for the transmission of useful signal without any interference. Accordingly, maximum degrees of freedom (DoFs) for the whole network can be achieved. The IA scheme is studied for many different networks, e.g., X channel [10], K -user interference channel (IC) [8, 11], heterogeneous networks [12–14], and cognitive radio networks [15, 16]. Moreover, the importance of the channel state information (CSI) for successful IA implementation is addressed in many works [17, 18]. Additionally, the feasibility conditions for IA implementation were the core of careful research studies [8–10].

Evaluating the capacity of a general IC is still a difficult goal for researchers in wireless communications and information theory [19] communities. However, IA technique is introduced as a DoFs optimal approach to interference management [10, 11]. This means that it can achieve the capacity of the IC at high SNR value. Note that IA approach can be achieved in time, frequency, and space dimensions. However, applying IA approach in the space dimension is the most popular due to the widespread use of MIMO technology. In MIMO networks, IA technique is applied using transmit beamforming matrices that help keeping all undesired received signals at each receiver within the same minimum dimensional sub-space, leaving the desired signal sub-spaces interference-free. Then, a receive beamforming matrix orthogonal to the interference sub-spaces at each receiver is used to completely eliminate the undesired interference signals [18, 20].

Recently, maximizing the capacity and accordingly the sum-rate for NOMA-based MU-MIMO communication networks becomes a target for many research works [21–24]. In [21], the problem of maximizing the

sum-rate for NOMA-based MIMO communication systems is studied under both total transmit power and minimum rate per user constraints. However, this study gives no attention to the applicability of successive interference cancellation (SIC) technique for networks with large number of users. In this work, they proposed PA scheme based on the CSI corresponding to full-rate transmission condition. The concept of signal alignment for both uplink and downlink transmissions in NOMA-based MIMO systems is addressed in [22]. Specifically, the authors used stochastic geometry to evaluate the performance of the proposed transmission framework with both randomly deployed users and interferers. The authors in [23] proposed a user-clustering algorithm for conventional NOMA-based MU-MIMO systems. They also investigated the performance of NOMA-based MIMO systems compared to OMA-based MIMO systems and concludes that NOMA-based MIMO systems are offering better capacity than the conventional OMA-based MIMO counterparts. Unlike our work, the method presented in [23] does not consider working with IA-based networks. In [24], the authors proposed a resource allocation scheme based on IA for NOMA-based networks. Specifically, they proposed a PA algorithm for 2-users NOMA network that implements the singular value decomposition (SVD)-based IA scheme which is not scalable to networks with large number of users. Additionally, they targeted optimizing the sum-rate under total power constraint. However, the generalization of the PA to the case where there are $K > 2$ users in the network is done in heuristically non-optimal manner based on 2-users pairing. Moreover, the solutions presented in [24] totally ignores the practical feasibility of SIC technique as well as the QoS requirements at each user, which are all considered in our proposed joint optimization algorithms.

In this article, we propose a joint IA and PA framework for optimizing the sum-rate of the NOMA-based MU-MIMO systems. The main contributions in our article can be summarized as follows:

- We propose a system and signal model for NOMA-based MU-MIMO systems that implements both the IA and PA techniques.
- We formulate the IA problem for NOMA-based MU-MIMO systems as an optimization problem and then find the optimum solutions according to the approach of IA employed for maximizing the system sum-rate.
- A PA technique for NOMA-based MU-MIMO system that employs IA transceivers is introduced, aiming to maximize the sum-rate under total power, robust SIC feasibility, and user QoS constraints.
- We devise three iterative algorithms for solving the optimization problem in the previous item, through

jointly optimizing the IA transceivers and PA coefficients of the system users.

- Compare the performance of the joint optimization-based iterative algorithms in both OMA and NOMA-based MU-MIMO systems.

The remaining sections are organized as follows: Section 2 introduces the signal and system model for the considered downlink NOMA-based MU-MIMO system. Then, different approaches for realizing the IA conditions for the downlink NOMA-based MU-MIMO systems with full CSI available at the base-station (BS) are addressed in Section 3 together with a simple solution for the case of no CSI available at the BS. This is followed by exploiting the role of both the optimum PA and clustering in maximizing the achievable sum-rate, in Section 4. Simulation results with their discussion are presented in Section 5, and Section 6 concludes our work.

Notation: Vectors and matrices are written in boldface lower-case and upper-case letters, respectively. The \mathbf{A}^\dagger and \mathbf{A}^* are referred to as the complex Hermitian transpose, and the complex conjugate of matrix \mathbf{A} , respectively. The symbols $\text{tr}(\mathbf{A})$ and $\|\mathbf{A}\|_2$ represent the trace and 2-norm of matrix \mathbf{A} , respectively. Moreover, $\|\mathbf{a}\|$ represents the absolute value for the vector \mathbf{a} . The matrix \mathbf{I}_n stands for the identity matrix of size $n \times n$. The $\mathbf{x} \sim \mathcal{CN}(\mu, \Sigma)$ means that \mathbf{x} is complex Gaussian distributed with mean μ and covariance matrix Σ . The expression $\sigma_{\max}^2(\mathbf{H})$ refers to the maximum eigenvalue of the matrix \mathbf{H} . The $\text{null}(\mathbf{A})$ refers to the null space of the matrix \mathbf{A} .

2 System and signal models

Consider a downlink MU-MIMO communication scenario where a BS with M transmit antennas is communicating with multiple UEs, each equipped with N receiving antennas. The served UEs are grouped into M clusters with K UEs in each cluster (Fig. 1). In this work, we are considering scenarios in which the number of antennas at each user, namely N , is greater than the number of antennas equipped at the BS, namely M , that is to say $N \geq M$. This assumption is popular in some 5G scenarios such as ultra-dense small cells and cloud-radio access networks (C-RANs) [2]. Through this assumption we are trying to consider some of the realistic scenarios that all 5G communities and mobile communication companies agreed that it will be challenging in the near future. One of the main pillars upon which the next generation mobile networks will be based for achieving the 1000 times capacity scaling is the ultra-dense small-cell networks. In such network design, low-power low-cost small-cell BSs will be employed for mobile data offloading. So, it is very likely that it owns the same number of antennas as the UE or even less, given the rapid progress in increasing the capabilities of such UEs. Another network design that support our assumption is the C-RANs, in which UEs are served

by a small number of low-cost remote radio heads (RRHs) to reduce the fronthaul overhead [2].

The power-domain multiplexed signal of the users' signals in cluster m is expressed as:

$$\tilde{\mathbf{s}}_m = \alpha_{m,1}s_{m,1} + \alpha_{m,2}s_{m,2} + \dots + \alpha_{m,K}s_{m,K}, \quad (1)$$

where $s_{m,k}$ is the useful information signal to be transmitted to the k^{th} user in the m^{th} cluster, and $\alpha_{m,k}$ is its corresponding NOMA PA coefficient. The signals to be transmitted by the BS in the downlink direction is firstly precoded using the beamforming filter $\mathbf{V} \in \mathbb{C}^{M \times M}$. Accordingly, the BS downlink transmitted signal can be written as:

$$\mathbf{x} = \mathbf{V}\tilde{\mathbf{s}}, \quad (2)$$

where $\mathbf{x} = [x_1 x_2 \dots x_M]^T \in \mathbb{C}^{M \times 1}$ is the combined signal transmitted from the BS to all users in different clusters, with $x_m = \sum_{k=1}^K \alpha_{m,k}s_{m,k}$ is the data to be transmitted from the BS to the m^{th} cluster (Fig. 1). Let the radio channel over which the BS transmits its signals is denoted as $\mathbf{H} = [\mathbf{H}_1^T \mathbf{H}_2^T \mathbf{H}_3^T \dots \mathbf{H}_M^T]^T \in \mathbb{C}^{MKN \times M}$, where $\mathbf{H}_m \in \mathbb{C}^{KN \times M}$ are the channels between the BS and users in cluster m which are all Rayleigh fading channels, and the channel between the BS and the k^{th} user in the m^{th} cluster is denoted as $\mathbf{H}_{m,k}$. The vector $\tilde{\mathbf{s}}$ represents the power-domain multiplexed signals for all the M clusters, which can be expressed in matrix form as:

$$\tilde{\mathbf{s}} = \begin{bmatrix} \tilde{s}_1 \\ \vdots \\ \tilde{s}_M \end{bmatrix} = \begin{bmatrix} \alpha_{1,1}s_{1,1} + \alpha_{1,2}s_{1,2} + \dots + \alpha_{1,K}s_{1,K} \\ \vdots \\ \alpha_{M,1}s_{M,1} + \alpha_{M,2}s_{M,2} + \dots + \alpha_{M,K}s_{M,K} \end{bmatrix}. \quad (3)$$

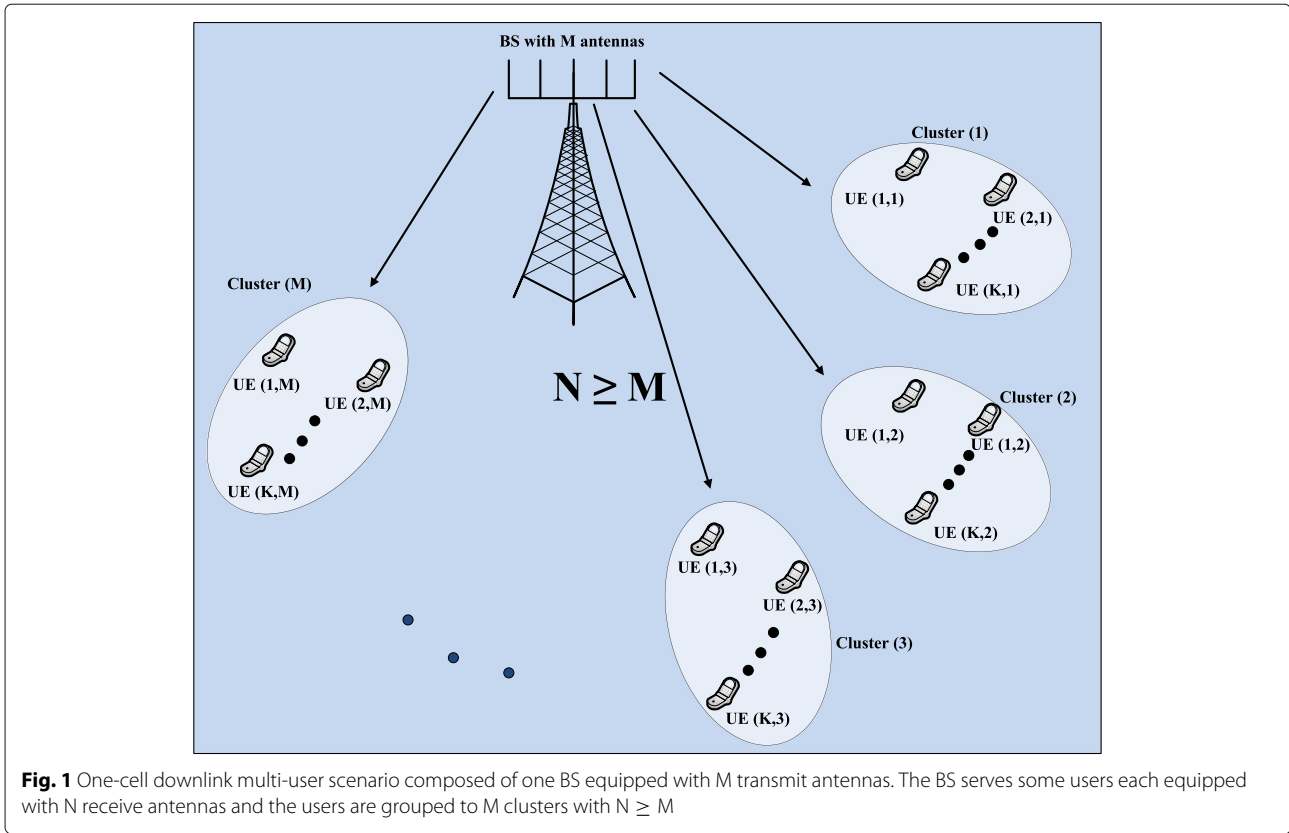
Accordingly, the signal received at the k^{th} user in the m^{th} cluster is decoded using $\mathbf{u}_{m,k}$ to give the detected signal as

$$\mathbf{u}_{m,k}^H \mathbf{y}_{m,k} = \mathbf{u}_{m,k}^H \mathbf{H}_{m,k} \mathbf{V} \tilde{\mathbf{s}} + \mathbf{u}_{m,k}^H \mathbf{n}_{m,k}. \quad (4)$$

Assuming that $\mathbf{V} = [\mathbf{v}_1 \mathbf{v}_2 \dots \mathbf{v}_M]$ and $\mathbf{U}_i = [\mathbf{u}_{i,1} \mathbf{u}_{i,2} \dots \mathbf{u}_{i,K}] \in \mathbb{C}^{N \times K}$, $\forall i \in \{1, 2, \dots, M\}$. The signal model in (4) can be rewritten as:

$$\mathbf{u}_{m,k}^H \mathbf{y}_{m,k} = \mathbf{u}_{m,k}^H \mathbf{H}_{m,k} \mathbf{v}_m (\alpha_{m,1}s_{m,1} + \dots + \alpha_{m,K}s_{m,K}) + \mathbf{u}_{m,k}^H \mathbf{H}_{m,k} \sum_{\substack{i=1 \\ i \neq m}}^M \mathbf{v}_i \tilde{\mathbf{s}}_i + \mathbf{u}_{m,k}^H \mathbf{n}_{m,k}. \quad (5)$$

The interference signals generated in the assumed scenario can be divided into two parts, namely, the intra-cluster interference and the inter-cluster interference. The intra-cluster interference results from the intentional overlapping/superimposing of signals that are to be



transmitted to users belonging to the cluster of the user of interest, namely, the self-interference generated due to the implementation of the NOMA technique. On the other hand, the inter-user interference originated due to the transmission of signals to users who are not belonging to the same cluster of the considered user. Using the notation of intra-cluster and inter-cluster interference, the signal model in (5) can be detailed as:

$$\begin{aligned}
 \mathbf{u}_{m,k}^H \mathbf{y}_{m,k} &= \underbrace{\mathbf{u}_{m,k}^H \mathbf{H}_{m,k} \mathbf{v}_m \alpha_{m,k} s_{m,k}}_{\text{Desired Signal}} + \underbrace{\mathbf{u}_{m,k}^H \mathbf{H}_{m,k} \sum_{\substack{j=1 \\ j \neq k}}^K \mathbf{v}_m \alpha_{m,j} s_{m,j}}_{\text{Intra-cluster Interference}} \\
 &+ \underbrace{\mathbf{u}_{m,k}^H \mathbf{H}_{m,k} \sum_{\substack{i=1 \\ i \neq m}}^M \mathbf{v}_i \tilde{s}_i}_{\text{Inter-cluster Interference}} + \underbrace{\mathbf{u}_{m,k}^H \mathbf{n}_{m,k}}_{\text{Noise}}. \tag{6}
 \end{aligned}$$

where $i, m \in \{1, 2, \dots, M\}$, and $j, k \in \{1, 2, \dots, K\}$. Equation (6) shows how IA and NOMA schemes are integrated together to optimize the sum-rate of MU-MIMO network. The IA technique is applied through implementing the transmit and receive beamformers, $\mathbf{u}_{m,k}$ and \mathbf{v}_m . On the other hand, NOMA is applied through superimposing the signals of all users in the cluster together using power domain multiplexing, and this is achieved through

careful evaluation of the PA coefficients. Our proposed algorithms will jointly optimize the beamforming vectors and the PA coefficients based on different objectives that are all related to the system sum-rate. The knowledge of the channel conditions is very critical for the implementation of NOMA systems. Accordingly and without loss of generality, we will assume the channels such that the effective channel gains are ordered as follows:

$$|\mathbf{u}_{m,1}^H \mathbf{H}_{m,1} \mathbf{v}_m|^2 \geq \dots \geq |\mathbf{u}_{m,K}^H \mathbf{H}_{m,K} \mathbf{v}_m|^2, \tag{7}$$

and according to the principles of NOMA technique, the PA coefficients of the users with in the m^{th} cluster are ordered as follow:

$$\alpha_{m,1}^2 \leq \dots \leq \alpha_{m,K}^2. \tag{8}$$

Based on (6), the signal-to-interference-plus-noise power (SINR) ratio for the K^{th} user, the user with smallest effective channel gain in the m^{th} cluster, is given by

$$\text{SINR}_{m,K} = \tag{9}$$

$$\frac{|\mathbf{u}_{m,K}^H \mathbf{H}_{m,K} \mathbf{v}_m|^2 \alpha_{m,K}^2}{\sum_{j=1}^{K-1} |\mathbf{u}_{m,K}^H \mathbf{H}_{m,K} \mathbf{v}_m|^2 \alpha_{m,j}^2 + \sum_{\substack{i=1 \\ i \neq m}}^M |\mathbf{u}_{m,K}^H \mathbf{H}_{m,K} \mathbf{v}_i|^2 + |\mathbf{u}_{m,K}|^2 \frac{1}{\rho}},$$

where ρ refers to the transmit SNR. According to the principles of the NOMA technique, the k^{th} user, $\forall 1 < k < K$ in the m^{th} cluster, needs to decode the messages sent to other users

with poorer channel conditions first before decoding its own message. Accordingly, the message $s_{m,j}$, $K \geq j \geq (k+1)$, can be detected at k^{th} user in the m^{th} cluster with SINR expressed as:

$$\text{SINR}_{m,k}^j = \frac{|\mathbf{u}_{m,k}^H \mathbf{H}_{m,k} \mathbf{v}_m|^2 \alpha_{m,j}^2}{\sum_{l=1}^{j-1} |\mathbf{u}_{m,k}^H \mathbf{H}_{m,k} \mathbf{v}_m|^2 \alpha_{m,l}^2 + \sum_{i=1, i \neq m}^M |\mathbf{u}_{m,k}^H \mathbf{H}_{m,k} \mathbf{v}_i|^2 + |\mathbf{u}_{m,k}|^2 \frac{1}{\rho}}. \quad (10)$$

It is the role of the SIC to remove the message $s_{m,j}$ from the observation of the k^{th} user. This message can be decoded successfully only when meeting the condition $\log(1 + \text{SINR}_{m,k}^j) > R_{m,j}$, with $R_{m,j}$ denoting the j^{th} user target data rate. The operation of the SIC technique will continue until the k^{th} user decodes its own message with SINR equals $\text{SINR}_{m,k}^k$. The first user in the m^{th} cluster, which is the user with largest effective channel gain, is responsible for decoding all the messages of other users in the cluster. If it is successful, it can decode its own message with SINR equals

$$\text{SINR}_{m,1}^1 = \frac{|\mathbf{u}_{m,1}^H \mathbf{H}_{m,1} \mathbf{v}_m|^2 \alpha_{m,1}^2}{\sum_{i=1, i \neq m}^M |\mathbf{u}_{m,1}^H \mathbf{H}_{m,1} \mathbf{v}_i|^2 + |\mathbf{u}_{m,1}|^2 \frac{1}{\rho}}. \quad (11)$$

IA and PA techniques are both used to improve the sum-rate for many different wireless communication scenarios [25]. However, up to the best of our knowledge, the study of combining IA approach with PA technique in NOMA-based MU-MIMO environment is not sufficiently conducted. In our proposed framework, the design of the PA scheme depends mainly on the IA strategy to be employed. So, the design of the precoding and decoding filters based on the principles of IA is accomplished first and consequently the PA strategies will be achieved. In the following section, the problem formulation for designing the IA-based precoding and decoding matrices for different IA approaches will be manipulated. This will be followed with the PA design problem which will be addressed in Section 4.

3 IA solutions for multi-user MIMO-NOMA

The design of the precoding and decoding filters for all the network nodes depends on the objective of the IA design process and the availability of the CSI. In this section, we consider the case where no global CSI available at the BS followed by the case with full global CSI available at the BS and IA transceivers design in each case. In our designs for NOMA-based MU-MIMO system with full global CSI at the BS, the considered objectives of IA technique are SINR maximization approach (max-SINR), interference leakage minimization approach (MIL), and sum-rate maximization approach (Max-SR). The derivations and details of each approach are discussed in the below subsections.

3.1 The case with no CSI available at the BS

In the proposed framework, the IA technique is responsible for removing the inter-cluster interference leaving the intra-cluster

interference to the SIC technique implicitly implemented in the NOMA design. Accordingly, the IA conditions that guarantee the removal of inter-cluster interference are expressed as follows:

$$\mathbf{u}_{m,k}^H \mathbf{H}_{m,k} \mathbf{v}_i = 0, \quad \forall i \neq m \quad (12)$$

The availability of CSI at the BS can be considered as a great system overhead. Accordingly, designing IA precoding and decoding filters with no CSI available at the BS, however, it is non-optimal, but it is considered in many practical scenarios because of its reduced system overhead of acquiring the global CSI from all the system nodes. One of the possible solutions to (12) is to choose \mathbf{V} , as $\mathbf{V} = \mathbf{I}_M$. Choosing \mathbf{V} in this form means that the BS broadcasts user messages without any processing, which reduces the overhead due to handshaking messages in acquiring and forwarding CSI in the network. Accordingly, the decoding filters can be evaluated by substituting in (12) as:

$$\mathbf{u}_{m,k}^H \mathbf{h}_{i,mk} = 0, \quad \forall i \neq m \quad (13)$$

where $\mathbf{h}_{i,mk}$ is the i^{th} column of $\mathbf{H}_{m,k}$. As a result of that, the IA constraints at the k^{th} user in the m^{th} cluster can be written as:

$$\mathbf{u}_{m,k}^H \underbrace{[\mathbf{h}_{1,mk} \cdots \mathbf{h}_{m-1,mk} \mathbf{h}_{m+1,mk} \cdots \mathbf{h}_{M,mk}]}_{\tilde{\mathbf{H}}_{m,k} \in \mathbb{C}^{N \times M}} = 0, \quad (14)$$

The above equation can be solved for $\mathbf{u}_{m,k}$ as:

$$\mathbf{u}_{m,k} = \text{null}(\tilde{\mathbf{H}}_{m,k}), \quad \forall k \in \{1, 2, \dots, K\}, \text{ and } m \in \{1, 2, \dots, M\} \quad (15)$$

By using the precoding and decoding matrices derived in this section, the inter-cluster interference will be eliminated, and the SINR for K^{th} user in the m^{th} cluster will be given by:

$$\text{SINR}_{m,K}^j = \frac{|\mathbf{u}_{m,K}^H \mathbf{h}_{m,mK}|^2 \alpha_{m,K}^2}{\sum_{j=1}^{K-1} |\mathbf{u}_{m,K}^H \mathbf{h}_{m,mK}|^2 \alpha_{m,j}^2 + |\mathbf{u}_{m,K}|^2 \frac{1}{\rho}}, \quad (16)$$

similarly, messages of users j , $K \geq j \geq k+1 \geq 1$ will be successfully detected at the k^{th} user, $K > k > 1$ with SINR:

$$\text{SINR}_{m,k}^j = \frac{|\mathbf{u}_{m,k}^H \mathbf{h}_{m,mk}|^2 \alpha_{m,j}^2}{\sum_{l=1}^{j-1} |\mathbf{u}_{m,k}^H \mathbf{h}_{m,mk}|^2 \alpha_{m,l}^2 + |\mathbf{u}_{m,k}|^2 \frac{1}{\rho}}, \quad (17)$$

The SIC scheme implemented with NOMA technique will take care of the remaining intra-cluster interference. Specifically, for the users k , and j , with $K \geq j \geq k+1 \geq 1$, when the message $s_{j,1}$ is successfully detected at the k^{th} user, it will be removed from the k^{th} user's superimposed received signal, and SIC scheme will continue working until its own message is received with SINR equals $\text{SINR}_{m,k}^k$. The evaluation of the optimum values of the PA coefficients will be discussed in Section 4.

3.2 The case with full global CSI available at the BS

In this section, we discuss different approaches for evaluating IA-based precoding and decoding filters according to the objective of the IA optimization problem. For each approach, we will formulate the optimization problem which is used at

the BS to determine the optimal IA transceiver design for all users and the BS. Specifically, we explain how to design the optimal IA precoder and decoder for each user-BS pair using the MIL, Max-SINR, and Max-SR approaches through solving their respective optimization problems. The general idea of using IA in our scenario is to align the unwanted received signals at the user of interest (the power multiplexed signals assigned to other clusters), into an interference subspace and reducing its projection within the desired signal subspace (the power multiplexed signals of users in its cluster). For example, for the k^{th} user in the m^{th} cluster, the IA constraints are:

$$\text{rank}(\mathbf{u}_{m,k}^H \mathbf{H}_{m,k} \mathbf{v}_m) = M, \tag{18}$$

$$\mathbf{u}_{m,k}^H \mathbf{H}_{m,k} \mathbf{v}_i = 0, \quad \forall i \neq m \tag{19}$$

$$\forall m \in \{1, 2, \dots, M\} \ \& \ k \in \{1, 2, \dots, K\}$$

IA is used to align the effect of all other clusters by considering them as interference and directing their effects into the interference subspace. This will leave each user only with the effect of its cluster-partners which can be dealt with the SIC technique which is already the core of the NOMA radio access technology.

3.2.1 Interference leakage minimization approach

As the name implies, this approach targets minimizing the other clusters-interference signals deliberated to the desired signal subspace at the user, and the process can be accomplished for the whole cluster at one shot by solving the corresponding optimization problem. The optimization problem corresponding to the m^{th} cluster is formulated as:

$$\underset{\{\mathbf{U}_m, \mathbf{V}\}}{\text{minimize}} \ l_m \tag{20}$$

$$\text{s.t. } \mathbf{U}_m \mathbf{U}_m^H = \mathbf{I}_N,$$

$$\mathbf{V} \mathbf{V}^H = \mathbf{I}_M,$$

where $l_m = \text{tr}[\mathbf{U}_m^H \mathbf{Q}_m \mathbf{U}_m]$ is the total interference leakage deliberated to the useful subspace of cluster m , and \mathbf{Q}_m is the interference covariance matrix for the m^{th} cluster, $\mathbf{Q}_m = \sum_{i=1; i \neq m}^M \sum_{k=1}^K \alpha_{m,k} \mathbf{H}_{m,k} \mathbf{V} \mathbf{V}^H \mathbf{H}_{m,k}^H$ [8]. This optimization problem can be solved by fixing a subset of variables (either \mathbf{U}_m or \mathbf{V}), and then optimize for the others, then alternate the roles between the fixed constant variables and the optimization variables. This technique tries to minimize interference leakage by alternatively optimizing the IA beamforming filters. Thus, at the BS, suppose the transmission is carried out in a specific communication direction, the optimization problem (20) is subject to $\mathbf{U}_m \mathbf{U}_m^H = \mathbf{I}_N$, where we optimize for the decoding filters \mathbf{U}_m . On the other hand, when the communication direction is reversed, the precoding and decoding filters are interchanged, and the optimization problem is now constrained to $\mathbf{V} \mathbf{V}^H = \mathbf{I}_M$ instead. If we denote d_m as $d_m = \min(M, N)$, the resulted optimization problem in each direction can be solved iteratively using alternative minimization by finding the d_m eigenvectors corresponding to smallest d_m number of eigenvalues of the interference covariance matrix \mathbf{Q}_m at each iteration [8]. Therefore, the d_m columns of \mathbf{U}_m are given by:

$$\mathbf{U}_m^{[d]} = v_d [\mathbf{Q}_m], \quad \forall d = \{1, \dots, d_m\} \tag{21}$$

where $v_d [\mathbf{A}]$ refers to the eigenvectors corresponding to the d smallest eigenvalues of \mathbf{A} .

3.2.2 Maximum-SINR approach

Another criteria that typically used as an objective to the IA design is the SINR-maximization approach. Specifically, the IA transceiver filters can be designed to maximize the SINR instead of only minimizing the interference leakage, where the MIL approach gives no attempt to maximize the desired signal power within the desired signal subspace. In other words, the MIL approach does not depend at all on the channels through which the desired signal arrives at the intended receiver. According to [8], the IA filters are obtained by:

$$\mathbf{u}_{m,k} = \frac{(\mathbf{B}_{m,k})^{-1} \mathbf{H}_{m,k} \mathbf{v}_m}{\|(\mathbf{B}_{m,k})^{-1} \mathbf{H}_{m,k} \mathbf{v}_m\|}, \tag{22}$$

where

$$\mathbf{B}_{m,k} = \sum_{i=1}^M \sum_{j=1}^K \alpha_{i,j}^2 \mathbf{H}_{i,j} \mathbf{v}_m \mathbf{v}_m^H \mathbf{H}_{i,j}^H - \alpha_{m,k}^2 \mathbf{H}_{m,k} \mathbf{v}_m \mathbf{v}_m^H \mathbf{H}_{m,k}^H - \mathbf{I}. \tag{23}$$

The last criteria and optimization problem that is used to design the IA transceiver filters at the BS is the sum-rate maximization. The goal is to design the optimum transceivers that maximize the sum-rate.

3.2.3 Sum-rate maximization approach

With this approach, we want to obtain the optimum transceiver filters that maximize the total system sum-rate. Accordingly, the optimization problem that will be implemented to evaluate the IA transceivers have the following form:

$$\underset{\{\mathbf{u}_{m,k}, \mathbf{v}_m\}}{\text{minimize}} \ R_{sum} = \sum_{m=1}^M \sum_{k=1}^K R_{m,k} \tag{24}$$

$$\text{s.t. } \mathbf{U}_m \mathbf{U}_m^H = \mathbf{I}_N,$$

$$\mathbf{V} \mathbf{V}^H = \mathbf{I}_M,$$

where $R_{m,k}$ represents the mutual information rate between the BS and the k^{th} user in the m^{th} cluster, and it is given by:

$$R_{m,k} = \log_2 \frac{\left| \mathbf{I} + \sum_{i=1}^M \sum_{k=1}^K \alpha_{i,k}^2 \mathbf{u}_{m,k}^H \mathbf{H}_{i,k} \mathbf{v}_i \mathbf{v}_i^H \mathbf{H}_{i,k}^H \mathbf{u}_{m,k} \right|}{\left| \mathbf{I} + \sum_{\substack{i=1, \\ i \neq m}}^M \sum_{k=1}^K \alpha_{i,k}^2 \mathbf{u}_{m,k}^H \mathbf{H}_{i,k} \mathbf{v}_i \mathbf{v}_i^H \mathbf{H}_{i,k}^H \mathbf{u}_{m,k} \right|}, \tag{25}$$

For solving the optimization problem in (24), we will use an iterative algorithm based on Riemannian optimization method [26], which can be considered as a generalization of the

standard euclidean optimization by formulating the optimization problem over smooth manifolds instead of the standard euclidean space [27–29]. The update rule for the IA iterative algorithm that based on maximizing the sum-rate is given by the Riemannian optimization over the Grassmann manifold and based on geodesics of a straight line in the euclidean space to the manifold. The update rule of the decoding matrix \mathbf{U}_m , $m \in \{1, 2, \dots, M\}$ over the Grassmann manifold Gr with gradient descent method is expressed as [27]:

$$\begin{aligned} \mathbf{U}_m^{n+1} &= \phi_{Gr}(\mathbf{U}_m^n, \text{grad}_{\mathbf{U}_m} R_{\text{sum}}, \mu), \\ &= \exp(\mu (\nabla R_{\text{sum}}(\mathbf{U}_m) \mathbf{U}_m^H - \mathbf{U}_m \nabla R_{\text{sum}}(\mathbf{U}_m)^H)) \mathbf{U}_m, \end{aligned} \quad (26)$$

$$(27)$$

where $\phi_{Gr}(\cdot)$ is the geodesic emanating from \mathbf{U}_m on the Grassmann manifolds Gr , $\mathbf{U}_m \in Gr$, in the direction of the gradient of the function R_{sum} , expressed as “ $\text{grad}_{\mathbf{U}_m} R_{\text{sum}}$ ”, and μ is the step size. The gradient, $\text{grad}_{\mathbf{U}_m} R_{\text{sum}}$, on the Grassmann manifold Gr is computed as:

$$\text{grad}_{\mathbf{U}_m}^{Gr} R_{\text{sum}} = \nabla R_{\text{sum}}(\mathbf{U}_m) - \mathbf{U}_m \mathbf{U}_m^H \nabla R_{\text{sum}}(\mathbf{U}_m). \quad (28)$$

The natural gradient of $R_{\text{sum}}(\mathbf{U}_m)$, expressed as $\nabla R_{\text{sum}}(\mathbf{U}_m)$ is a real valued function. However, \mathbf{U}_m is a matrix whose components are complex, so according to [30], the gradient can be evaluated as

$$\nabla R_{\text{sum}}(\mathbf{U}_m) = 2 \frac{\delta(R_{\text{sum}}(\mathbf{U}_m))}{\delta \mathbf{U}_m^*} = 2 \left(\frac{\delta(R_{\text{sum}}(\mathbf{U}_m))}{\delta \mathbf{U}_m} \right)^* \quad (29)$$

$$\begin{aligned} &= \frac{2}{\ln 2} \sum_{i=1}^M \sum_{k=1}^K \alpha_{i,k} \mathbf{U}_m \mathbf{H}_{i,k}^H \mathbf{X}_i^{-1} \mathbf{H}_{i,k} \\ &- \frac{2}{\ln 2} \sum_{\substack{i=1, \\ i \neq m}}^M \sum_{k=1}^K \alpha_{i,k} \mathbf{U}_m \mathbf{H}_{i,k}^H \mathbf{Y}_i^{-1} \mathbf{H}_{i,k}, \end{aligned} \quad (30)$$

where $\frac{\delta(f(x))}{\delta x}$ refers to the partial derivative of the function $f(x)$ with respect to x . The matrices \mathbf{X} and \mathbf{Y} are expressed as:

$$\begin{aligned} \mathbf{X}_m &= \mathbf{I} + \sum_{i=1}^M \sum_{k=1}^K \alpha_{i,k} \mathbf{U}_m^H \mathbf{H}_{i,k} \mathbf{H}_{i,k}^H \mathbf{U}_m. \\ \mathbf{Y}_m &= \mathbf{I} + \sum_{\substack{i=1, \\ i \neq m}}^M \sum_{k=1}^K \alpha_{i,k} \mathbf{U}_m^H \mathbf{H}_{i,k} \mathbf{H}_{i,k}^H \mathbf{U}_m. \end{aligned}$$

The update rule for the iterative algorithm that computes the decoding matrices \mathbf{U}_m is derived by substituting (28) and (30) in (27).

4 The proposed joint PA and IA methods

In this section, the applied user clustering models are first explained; then, the concepts and details of the proposed PA algorithms are manipulated. Finally, the proposed joint PA and IA algorithms is proposed based on both the clustering and PA concepts.

4.1 User clustering models

User pairing is demonstrated to be very beneficial for the implementation of the NOMA technique in downlink MU scenarios [2]. In a similar fashion, we will illustrate the gain of grouping the users into clusters in the case of downlink NOMA-based MU-MIMO system with the implementation of joint IA and PA optimization. The clustering process and its optimization is beyond the scope of this article. However, we will implement two extreme models for user clustering to prove the importance of using it, in terms of sum-rate, when dealing with IA and PA for downlink NOMA-based MU-MIMO systems. The first model depends on grouping the K users with the best channels together in the first cluster, then the following K best channels' users are grouped within the second cluster, and so on. On the other hand, the second model depends on distributing the M users with best channel gains, one in each of the M clusters, then the following M best channels is distributed in the same fashion, and so on. Figure 2 illustrates the concepts of the two clustering models. In the following discussion, we will refer to the first and second models as the best-with-best and the best-with-poor models, respectively. In both clustering models, the user with the best channel gain can be considered as the cluster head.

4.2 Power allocation approach

We consider that the downlink NOMA-based MU-MIMO system is divided into clusters and the beamforming process is designed such that a single beam used to send all the data messages to their respective users within a specific cluster. Since each cluster contains the same number of users and their channel gains follow the same random distribution, we assume the power budget of the BS will be divided equally between all the clusters. If we assume that the power budget of the BS is denoted as P_{BS} , subsequently, this power is allocated equally between the M clusters with each cluster allocated an amount equal to (P_{BS}/M) . The power budget for each cluster will be allocated among the scheduled users within the cluster according to the principles of the NOMA technique. For the PA among the users within the cluster, the sum-rate is maximized under cluster power budget constraints, minimum user sum-rate (as quality of service metric) constraints, and constraints related to the implementation of SIC technique, i.e. minimum power differences among NOMA received signals as illustrated in [31]. The PA strategy will be applied separately with each cluster. Without loss of generality, we assume that the effective channel gains of the users within the m^{th} cluster satisfying $|\mathbf{u}_{m,1} \mathbf{H}_{m,1} \mathbf{V}_m| > |\mathbf{u}_{m,2} \mathbf{H}_{m,2} \mathbf{V}_m| > \dots > |\mathbf{u}_{m,k} \mathbf{H}_{m,k} \mathbf{V}_m| > \dots > |\mathbf{u}_{m,K} \mathbf{H}_{m,K} \mathbf{V}_m|$. Additionally, we refer to the minimum sum-rate values that must be guaranteed by all users within the cluster as $R_{m,1}, R_{m,2}, \dots, R_{m,K}$ where $R_{m,k} > 0, \forall m$ and $\forall k$. Since we are choosing the number of clusters equal to the number of transmitting antennas at the BS, each cluster will

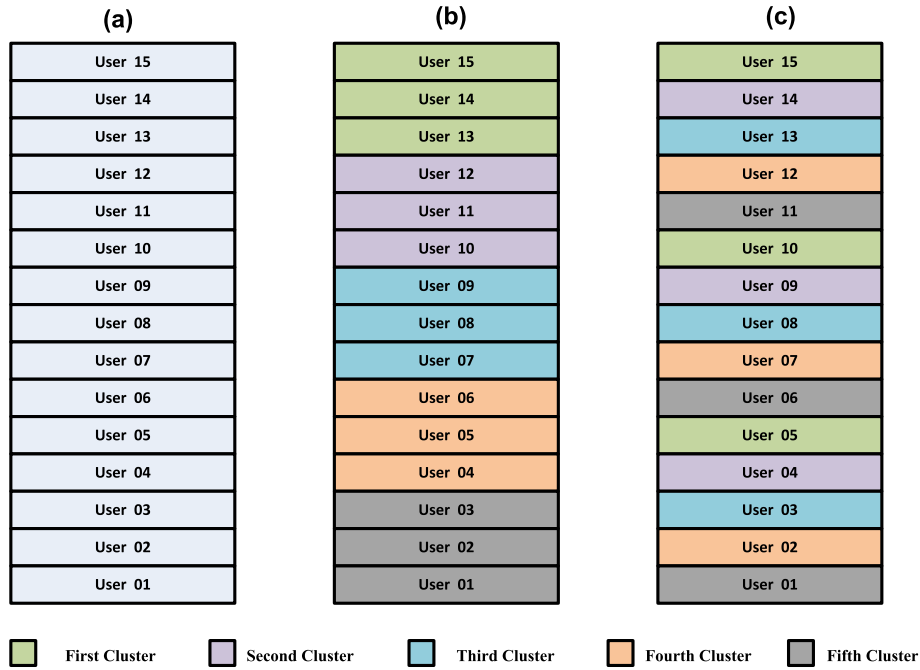


Fig. 2 The clustering models for downlink multi-user MIMO-NOMA with joint IA and PA optimization: **a** The users' effective channel gains are ordered in descending fashion. **b** The users are clustered according to the best-with-best model. **c** The users are clustered according to the best-with-poor model

use the whole system bandwidth BW to serve its users. The PA optimization problem for the users within the m^{th} cluster can be reformulated as:

$$\begin{aligned}
 & \text{maximize } \sum_{k=1}^K \text{BW} \log_2 \left(1 + \frac{\alpha_{m,k}^2 |\mathbf{u}_{m,k} \mathbf{H}_{m,k} \mathbf{V}_m|^2}{|\mathbf{u}_{m,k} \mathbf{H}_{m,k} \mathbf{V}_m|^2 \sum_{j=1}^{k-1} \alpha_{m,j}^2 + 1/\rho} \right) \\
 & \text{s.t. : } \quad \mathbf{C}_1 : \sum_{k=1}^K \alpha_{m,k}^2 \leq 1, \\
 & \quad \mathbf{C}_2 : \text{BW} \log_2 \left(1 + \frac{\alpha_{m,k}^2 |\mathbf{u}_{m,k} \mathbf{H}_{m,k} \mathbf{V}_m|^2}{|\mathbf{u}_{m,k} \mathbf{H}_{m,k} \mathbf{V}_m|^2 \sum_{j=1}^{k-1} \alpha_{m,j}^2 + 1/\rho} \right) \\
 & \quad \quad \geq R_{m,k}, \forall k \\
 & \quad \mathbf{C}_3 : \left(\alpha_{m,k}^2 - \sum_{j=1}^{k-1} \alpha_{m,j}^2 \right) |\mathbf{u}_{m,k-1} \mathbf{H}_{m,k-1} \mathbf{V}_m|^2 \\
 & \quad \quad \geq P_{th}, \forall k \neq 1
 \end{aligned} \tag{31}$$

where P_{th} denotes the threshold minimum received power difference between users' signals required for carrying out the SIC technique. The previous optimization problem is similar in notation to those mentioned in [31, 32], and accordingly the closed form solution presented in [32] can be applied directly to solve the optimization problem in (31). Let B and C denote the complementary set of users in the m^{th} cluster that meet the minimum sum-rate for the users and SIC visibility constraints, respectively. The optimal PA for the first user within the m^{th} cluster is given by:

$$\begin{aligned}
 \alpha_{m,1}^2 = & \frac{1}{\prod_{\substack{j=2 \\ j \notin B}}^K 2^{\lfloor \frac{R_{m,j}}{BW} \rfloor} \prod_{\substack{j=2 \\ j \in B}}^K 2} - \sum_{\substack{j=2 \\ j \notin B}}^K \frac{\left(2^{\lfloor \frac{R_{m,j}}{BW} \rfloor} - 1 \right)}{\left(\frac{P_{BS}}{M} \right) |\mathbf{u}_{m,j} \mathbf{H}_{m,j} \mathbf{V}_m|^2 \prod_{\substack{i=2 \\ i \notin B}}^j 2^{\lfloor \frac{R_{m,i}}{BW} \rfloor} \prod_{\substack{i=2 \\ i \in B}}^j 2} \\
 & - \sum_{\substack{j=2 \\ j \notin C}}^K \frac{P_{th}}{\left(\frac{2P_{BS}}{M} \right) |\mathbf{u}_{m,j-1} \mathbf{H}_{m,j-1} \mathbf{V}_m|^2 \prod_{\substack{i=2 \\ i \notin B}}^{j-1} 2^{\lfloor \frac{R_{m,i}}{BW} \rfloor} \prod_{\substack{i=2 \\ i \in B}}^{j-1} 2} }
 \end{aligned} \tag{32}$$

Additionally, the PA coefficient for the k^{th} user, with $k \neq 1$, within the m^{th} cluster can be expressed as:

- If $k \notin B$

$$\begin{aligned}
 \alpha_{m,k}^2 = & \left[\frac{1}{\prod_{\substack{j=k \\ j \notin B}}^K 2^{\lfloor \frac{R_{m,j}}{BW} \rfloor} \prod_{\substack{j=k \\ j \in B}}^K 2} - \sum_{\substack{j=k \\ j \notin B}}^K \frac{\left(2^{\lfloor \frac{R_{m,j}}{BW} \rfloor} - 1 \right)}{\left(\frac{P_{BS}}{M} \right) |\mathbf{u}_{m,j} \mathbf{H}_{m,j} \mathbf{V}_m|^2 \prod_{\substack{i=k \\ i \notin B}}^j 2^{\lfloor \frac{R_{m,i}}{BW} \rfloor} \prod_{\substack{i=k \\ i \in B}}^j 2} \right. \\
 & - \sum_{\substack{j=k \\ j \notin C}}^K \frac{P_{th}}{\left(\frac{2P_{BS}}{M} \right) |\mathbf{u}_{m,j-1} \mathbf{H}_{m,j-1} \mathbf{V}_m|^2 \prod_{\substack{i=k \\ i \notin B}}^{j-1} 2^{\lfloor \frac{R_{m,i}}{BW} \rfloor} \prod_{\substack{i=k \\ i \in B}}^{j-1} 2} } \\
 & \left. + \frac{1}{\left(\frac{P_{BS}}{M} \right) |\mathbf{u}_{m,k} \mathbf{H}_{m,k} \mathbf{V}_m|^2} \right] \times \left(2^{\lfloor \frac{R_{m,k}}{BW} \rfloor} - 1 \right).
 \end{aligned} \tag{33}$$

- If $k \in B$

$$\alpha_{m,k}^2 = \frac{1}{\prod_{j=k}^K 2^{\lfloor \frac{R_{m,j}}{BW} \rfloor} \prod_{j \in B} 2^{\lfloor \frac{R_{m,j}}{BW} \rfloor}} - \sum_{j=k}^K \frac{\left(2^{\lfloor \frac{R_{m,j}}{BW} \rfloor} - 1 \right)}{\left(\frac{P_{BS}}{M} \right) |\mathbf{u}_{m,j} \mathbf{H}_{m,j} \mathbf{V}_m|^2 \prod_{i \neq B}^j 2^{\lfloor \frac{R_{m,i}}{BW} \rfloor} \prod_{i \in B}^j 2} - \sum_{j \in C}^K \frac{P_{th}}{\left(\frac{2P_{BS}}{M} \right) |\mathbf{u}_{m,j-1} \mathbf{H}_{m,j-1} \mathbf{V}_m|^2 \prod_{i \neq B}^{j-1} 2^{\lfloor \frac{R_{m,i}}{BW} \rfloor} \prod_{i \in B}^{j-1} 2} + \frac{P_{th}}{\left(\frac{P_{BS}}{M} \right) |\mathbf{u}_{m,k-1} \mathbf{H}_{m,k-1} \mathbf{V}_m|^2} \quad (34)$$

The detailed steps for the proposed joint IA and PA framework based on different IA approaches are given in Algorithms 1, 2, and 3.

Algorithm 1 The MIL based IA approach for NOMA-based MU-MIMO systems

- 1: Initialize the beamforming filters, \mathbf{V}_m , $\forall m \in \{1, 2, \dots, M\}$, for the clusters with unitary matrices, and initialize the PA coefficients $\alpha_{m,k}$, $\forall m \in \{1, 2, \dots, M\}$, and $k \in \{1, 2, \dots, K\}$ while keeping the NOMA PA constraints.
- 2: Calculate the interference covariance matrix for each cluster, m , as:

$$\mathbf{Q}_m = \sum_{i=1; i \neq m}^M \sum_{k=1}^K \alpha_{m,k} \mathbf{H}_{m,k} \mathbf{V}_m \mathbf{V}_m^H \mathbf{H}_{m,k}^H$$

- 3: Compute the decoding matrices that minimize the interference leakage due to undesired messages, \mathbf{U}_m , according to (21).
- 4: Compute the beamforming matrices using Steps 2 and 3, where we assume a reverse communication direction and initializing the decoding matrices by the values obtained in the previous step and replace the decoding matrices with the beamforming matrices and vice-versa.
- 5: Update the PA coefficients for all users using (32), (33), and (34).
- 6: Repeat the Steps from 2 to 5 until the algorithm convergences.
- 7: Distribute the calculated transceiver filters, and the PA coefficients to the corresponding users.

Note that the PA coefficients are initialized in all the three algorithms as $\alpha_{m,k} = 1/K$. Each of the algorithms is dependent on a specific criteria for achieving the IA conditions as explained in Subsection 3.2. All these algorithms rely on the availability of CSI, and all apply the same power allocation algorithm introduced in Section 4. Since the evaluation of the

Algorithm 2 The Max-SINR based IA approach for NOMA-based MU-MIMO systems

- 1: Initialize the beamforming filters, \mathbf{V}_m , $\forall m \in \{1, 2, \dots, M\}$, for the clusters with unitary matrices, and initialize the PA coefficients $\alpha_{m,k}$, $\forall m \in \{1, 2, \dots, M\}$, and $k \in \{1, 2, \dots, K\}$ while keeping the NOMA PA constraints.
- 2: Calculate the matrix $\mathbf{B}_{m,k}$ for each user using (23).
- 3: Compute the decoding matrices that maximize the SINR, \mathbf{U}_m , according to (22).
- 4: Compute the decoding matrices using Steps 2 and 3, where we assume a reverse communication direction and initializing the decoding matrices by the values obtained in the previous step and replace the decoding matrices with the beamforming matrices and vice-versa.
- 5: Update the PA coefficients for all users using (32), (33), and (34).
- 6: Repeat the Steps from 2 to 5 until the algorithm convergences.
- 7: Distribute the calculated transceiver filters, and the PA coefficients to the corresponding users.

Algorithm 3 The Max-SR based IA approach for NOMA-based MU-MIMO systems

- 1: Initialize the beamforming filters, \mathbf{V}_m , $\forall m \in \{1, 2, \dots, M\}$, for the clusters with unitary matrices, the step size μ with 0.1, and initialize the PA coefficients $\alpha_{m,k}$, $\forall m \in \{1, 2, \dots, M\}$, and $k \in \{1, 2, \dots, K\}$ while keeping the NOMA PA constraints.
- 2: Calculate the matrix $\mathbf{B}_{m,k}$ for each user using (23).
- 3: Compute the decoding matrices that maximize the SINR, \mathbf{U}_m , according to (22).
- 4: Update the beamforming matrices, \mathbf{V}_m along the geodesic over the Grassmann manifold in the direction given by the gradient of R_{sum} using (27) and (30).
- 5: Update the PA coefficients for all users using (32), (33), and (34).
- 6: Update the optimization step size $\mu = \mu \times 0.95$.
- 7: Repeat the Steps from 2 to 6 in the reverse communication direction until the algorithm convergences.
- 8: Distribute the calculated transceiver filters, and the PA coefficients to the corresponding users.

matrices \mathbf{Q}_m , and $\mathbf{B}_{m,k}$ depends on the PA coefficients, the PA coefficients accordingly affect the design of the transmit and decode beamforming matrices. As a result, the proposed algorithms are jointly optimizing both the PA coefficients and the transceiver filters aiming to eventually optimize the system sum-rate. The joint optimization is solved under total power budget, user QoS, and robust SIC constraints as explained

in details in Section 4. It is worth noting that the proposed iterative IA techniques are carried out offline as we are assuming stationary block fading channels, which remains constant during the transmission process. Accordingly, the complexity analysis of the algorithms is not as important as the gain in the system sum-rate.

5 Simulation results and discussion

In this section, we introduce simulation results to illustrate the sum-rate improvement resulted due to joint optimization of IA transceivers and PA coefficients for downlink NOMA-based MU-MIMO systems. Additionally, the simulation results for the proposed NOMA-based MU-MIMO system with joint IA and PA optimization is compared with those of the conventional NOMA-based MU-MIMO as well as the OMA-based MU-MIMO systems. The channels between the BS and the users are all assumed to be Gaussian distributed Rayleigh fading with zero mean and unit variance in addition to the shadowing and the pathloss effects with parameters as mentioned in [32]. Additionally, we assume that perfect full global CSI is available at the BS. In other words, the BS owns a copy of the channel between it and each user in the system [8–18, 32]. The simulation results are obtained through averaging the measurements over 5000 channel realizations. For the proposed NOMA-based MU-MIMO network with clustering model employed, we have assumed that the number of clusters in the system equals the number of antennas at the BS, and all clusters have the same size (number of users in the cluster). A list of all the simulation parameters used in evaluating our results are in Table 1. The algorithms that will be involved in the comparison are MIL-IA implemented in OMA-based MU-MIMO system (MIL-IA-MIMO-OMA), MIL-IA implemented in conventional NOMA-based MU-MIMO system (MIL-IA-Conv-MIMO-NOMA), MIL-IA implemented in the proposed NOMA-based MU-MIMO system (MIL-IA-Proposed-MIMO-NOMA), Max-SINR-IA implemented in OMA-based MU-MIMO system (Max-SINR-IA-MIMO-OMA), Max-SINR-IA implemented in conventional NOMA-based MU-MIMO system (Max-SINR-IA-Conv-MIMO-NOMA), Max-SINR-IA implemented in the proposed NOMA-based MU-MIMO system (Max-SINR-IA-Proposed-MIMO-NOMA), Max-SR-IA implemented in OMA-based MU-MIMO system (Max-SR-IA-MIMO-OMA), Max-SR-IA implemented in conventional NOMA-based MU-MIMO system (Max-SR-IA-Conv-MIMO-NOMA), Max-SR-IA implemented in the proposed NOMA-based MU-MIMO (Max-SR-IA-Proposed-MIMO-NOMA), SVD-based IA implemented in OMA-based MU-MIMO (SVD-IA-MIMO-OMA), SVD-based IA implemented in conventional NOMA-based MU-MIMO system introduced in [24] (SVD-IA-Conv-MIMO-NOMA in [24]), SVD-based IA implemented in the proposed NOMA-based MU-MIMO system (SVD-IA-Proposed-MIMO-NOMA), and the conventional NOMA-based MU-MIMO system without IA (Conv-NOMA without IA [23]).

Figure 3 shows the variation of the sum-rate versus the transmitted power, P_{tr} , with different IA approaches for the proposed NOMA-based MU-MIMO as well as the conventional

Table 1 Simulation parameters

| Parameter name | Value |
|--|------------------------------|
| System effective bandwidth (BW) | 20 MHz |
| Bandwidth of a resource block | 200 KHz |
| Number of available resource blocks | 100 |
| Transmit power budget | 46 dBm |
| Detection threshold at SIC receiver (P_{th}) | 10 dBm |
| Cell diameter | 600 m |
| Path-loss Exponent | 4 |
| Noise power density (N_0) | − 174 dBm/Hz |
| No. of users per cluster (K) | 4 |
| No. of transmitting antennas (M) | 2 |
| No. of receiving antennas (N) | 4 |
| Shadowing standard deviation | 8 dB |
| Path-loss equation at 2 GHz band | $15.3 + 37.6 \log_{10}(d_0)$ |
| Initial power allocation coefficients ($\alpha_{m,k}^2$) | 1/K |

MIMO-NOMA and MIMO-OMA systems. In these simulation results, we have assumed that users having the same order within the clusters will be assigned the same minimum sum-rate value, which is inserted in (31) as the minimum sum-rate constraint, mathematically speaking, we assume that $R_{m-1,k} = R_{m,k} = R_{m+1,k}$, $\forall m \in \{1, 2, \dots, M\}$. It is obvious from the results that, the IA approach that depends on maximizing the system sum-rate over the Grassmann manifold outperforms both the MIL and Max-SINR approaches with both the proposed and the conventional systems. The cause behind that fact is that the sum-rate maximization approach considers optimizing all the Shannon's capacity equation's parameters, namely the spatial DoFs, desired signal power, and the undesired interference power, while other approaches consider optimizing only one or two of these parameters. Additionally, the proposed NOMA-based MU-MIMO system that employs clustering, IA, and optimum PA obtained by solving (31) provides the most higher sum-rate performance, followed by the conventional NOMA-based MU-MIMO system, and the OMA-based MU-MIMO system provides the worst performance in the comparison. Moreover, it is obvious that all the proposed algorithms outperform the state-of-the-art algorithms [23, 24].

Figure 4 shows the effect of choosing the clustering model within the proposed NOMA-based MU-MIMO system. In our work, we employed the two clustering models shown in Fig. 2. It is very clear from the results that the proposed NOMA-based MU-MIMO system performs better with the best-with-poor clustering model than with the case of best-with-best clustering model. This is due to the effectiveness of the SIC technique with the best-with-poor model than with the best-with-best model. In other words, the clustering model somehow governs and keeps the minimum received power differences among the signals of different users with the NOMA-based MU-MIMO system improving the performance of the SIC technique and accordingly provides optimum interference cancellation within

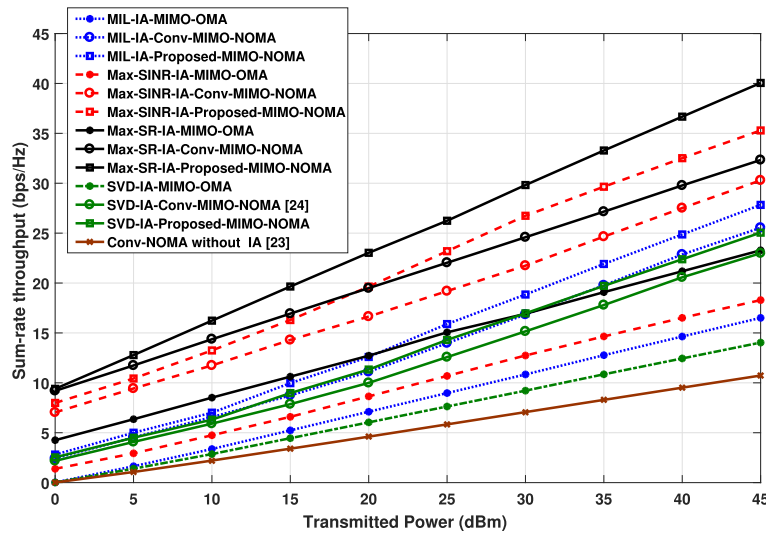


Fig. 3 The transmitted power P_{tr} in (dBm) versus the sum-rate in (bits/sec/Hz) for the proposed MIMO-NOMA approach (With joint IA and PA), in comparison with the conventional MIMO-NOMA approach (no clustering and the power distributed equally between users), and the case of IA with MIMO-OMA

the cluster. Another important observation is that the superiority of the best-with-poor clustering model than the best-with-best clustering model is guaranteed with any of the IA approaches. At a transmitted power of 35 dB, the proposed MIMO-NOMA with Max-SR IA approach achieves around 11 (bits\sec\Hz) more sum-rate with best-with-poor clustering model than with best-with-best model. Similar conclusions can be reported with other IA approaches at different transmitted power levels.

Figure 5 shows the effect of the cluster size, defined as the number of users per cluster, on the system sum-rate. The sum-rate grows almost linearly with the cluster size for all IA

approaches until reaching a specific cluster size, 10 and 12 users at transmission power levels 15dBm and 35dBm, respectively. After that, the sum-rate begins to decay due to the lower efficiency of the SIC technique and accordingly the growth of intra-cluster interference. In other words, the sum-rate for the NOMA-based MU-MIMO system grows with the cluster size as long as the system meets the constraint of minimum received power differences among the users. Once the system violates this constraint, the SIC technique provides lower efficiency in canceling the intra-cluster interference and the sum-rate begins to decrease. This behavior is common among all IA approaches with different transmission powers.

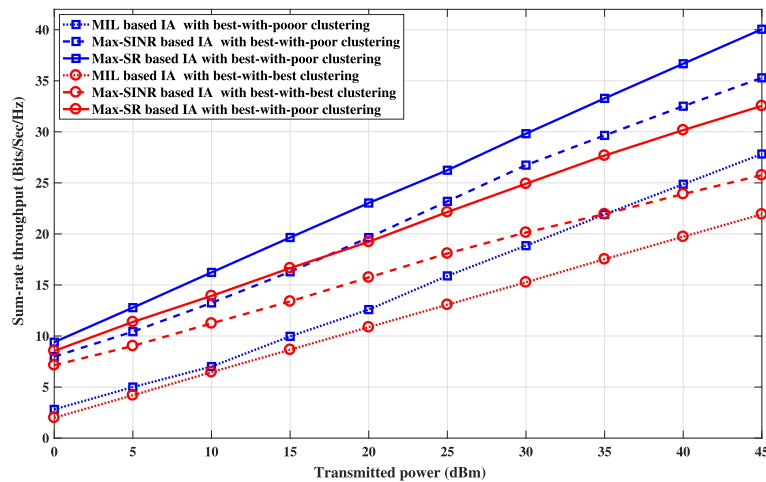


Fig. 4 The transmitted power in (dBm) versus the sum-rate in (Bits/sec/Hz) for the proposed MIMO-NOMA approach (with joint IA and PA) with different IA approaches and different clustering models

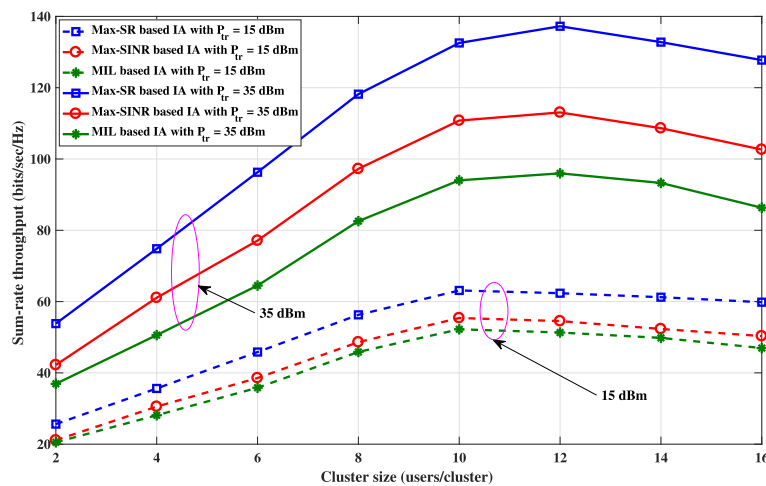


Fig. 5 The cluster size in (users/cluster) versus the sum-rate in (Bits/sec/Hz) for different IA approaches with the proposed MIMO-NOMA with transmitted power of 15dBm, and 35dBm

6 Conclusions

In this article, we have studied the application of different IA approaches to downlink NOMA-based MU-MIMO systems. Specifically, we have proposed a joint IA and PA framework for maximizing the sum-rate of the NOMA-based MU-MIMO system under different approaches of IA. It turns out from the simulation results that IA is still an excellent scheme for accessing the maximum DoFs of the next generation NOMA-based networks. Additionally, user clustering is proven to be a critical step for the joint optimization of the PA coefficients and IA transceivers in NOMA-based MU-MIMO systems. Finally, we concluded that accompanying the NOMA access technology with IA combined with optimum PA algorithm can be considered as a key solution for achieving the capacity scaling targeted by next generation 5G networks. As a future work, the performance of the proposed algorithms would be studied under both instantaneous and statistical CSI. Moreover, the performance of the IA-based transceivers in NOMA-based MU-MIMO system will be investigated with partial CSI.

Abbreviations

BS: Base-station; CSI: Channel state information; C-RAN: Cloud-radio access networks; DoFs: Degrees of freedom; IA: Interference alignment; IC: Interference channel; MU-MIMO: Multi-user multiple-input multiple-output; NOMA: Non-orthogonal multiple access; OMA: Orthogonal multiple access; PA: Power allocation; QoS: Quality of service; RRH: Remote radio heads; SIC: Successive interference cancellation; SINR: Signal to interference plus noise ratio; SNR: Signal to noise ratio; SVD: Singular value decomposition; UE: User equipment; 5G: Fifth generation

Acknowledgements

The authors would like to thank the anonymous reviewers for their insightful comments.

Funding

The EURASIP Journal on Wireless Communications and Networking supports the publication of this article.

Authors' contributions

All authors discussed the experiments; MR performed the experiments and wrote the paper. LH and PZ have made some useful comments on the paper. All authors have read and approved the final manuscript.

Competing interests

The authors declare that they have no competing interests.

Publisher's Note

Springer Nature remains neutral with regard to jurisdictional claims in published maps and institutional affiliations.

Author details

¹Multi-dimensional Signal Processing Lab., College of Information Engineering, Shenzhen University, Shenzhen, China. ²Department of Electronics and Communication Engineering, Faculty of Electronic Engineering, Menoufia University, Shibin Al-Kawm 21974, Egypt.

Received: 5 February 2018 Accepted: 8 August 2018

Published online: 04 September 2018

References

- L. Dai, B. Wang, Z. Ding, Z. Wang, S. Chen, L. Hanzo, A Survey of Non-Orthogonal Multiple Access for 5G. *IEEE Surv. Tutor.* Accessed on 8 July 2018. [Online]. available <https://doi.org/10.1109/COMST.2018.2835558>
- Z. Ding, F. Adachi, V. Poor, The application of MIMO to non-orthogonal multiple access. *IEEE Trans. Wirel. Commun.* **15**(1), 537–552 (2016)
- Z. Ding, X. Lei, G.K. Karagiannidis, R. Schober, J. Yuan, V.K. Bhargava, A Survey on Non-Orthogonal Multiple Access for 5G Networks: Research Challenges and Future Trends. *IEEE J. Sel. Areas Commun.* **35**(10), 2181–2195 (2017)
- S. Timotheou, I. Krikidis, Fairness for non-orthogonal multiple access in 5G systems. *IEEE Signal Sig. Process.* **22**(10), 1647–1651 (2015)
- L. Dai, B. Wang, Y. Yuan, S. Han, I. Chih-lin, Z. Wang, Non-orthogonal multiple access for 5G: solutions, challenges, opportunities, and future research trends. *IEEE Commun. Mag.* **53**(9), 74–81 (2015)
- L. Lv, Q. Ni, Z. Ding, J. Chen, Application of non-orthogonal multiple access in cooperative spectrum-sharing networks over Nakagami- m fading channels. *IEEE Trans. Veh. Technol.* **66**(06), 5506–5511 (2016)
- S. Islam, M. Zeng, O. Dobre, K. Kwak, Resource Allocation for Downlink NOMA Systems: Key Techniques and Open Issues. *IEEE Wirel. Commun.* **25**(2), 40–47 (2018)
- K. Gomadam, V.R. Cadambe, S.A. Jafar, A distributed numerical approach to interference alignment and applications to wireless interference networks. *IEEE Trans. Inf. Theory.* **57**(06), 3309–3322 (2011)
- O. El Ayach, S.W. Peters, R.W. Heath Jr., The feasibility of interference alignment over measured MIMO-OFDM channels. *IEEE Trans. Veh. Technol.* **59**(09), 4309–4321 (2010)

10. T. Ying, W. Feng, G. Liu, Space-Time Interference Alignment: DoF of Two-User MIMO X-Channel with Alternating CSIT. *IEEE Commun. Lett.* **21**(5), 1167–1170 (2017)
11. X. Jing, L. Mo, H. Liu, C. Zhang, Linear Space-Time Interference Alignment for K-User MIMO Interference Channel. *IEEE Access.* **6**, 3085–3095 (2017)
12. M. Rihan, M. Elsabrouty, O. Muta, H. Furukawa, in *IEEE vehicular technology conference (VTC Spring)*. Interference alignment with limited feedback for macrocell-femtocell heterogeneous networks (IEEE, Glasgow, 2015), pp. 1–5
13. M. Rihan, M. Elsabrouty, O. Muta, H. Furukawa, Interference mitigation framework based on interference alignment for femtocell-macrocell two tier cellular systems. *IEICE Trans. Commun.* **E98-B**(03), 467–476 (2015)
14. T.T. Vu, H.H. Kha, O. Muta, M. Rihan, Energy-efficient interference mitigation with hierarchical partial coordination for MIMO heterogeneous networks. *IEICE Trans. Commun.* **E100-B**(06), 3247–3255 (2016)
15. H. Men, N. Zhao, M. Jin, J. M. Kim, Optimal transceiver design for interference alignment based cognitive radio networks. *IEEE Commun. Lett.* **19**(08), 1442–1445 (2015)
16. B. Guler, A. Yener, Selective interference alignment for MIMO cognitive femtocell networks. *IEEE J. Sel. Areas Commun.* **32**(03), 439–450 (2014)
17. S. Cho, K. Huang, D.K. Kim, V.K.N. Lau, H. Chae, H. Seo, B. Kim, Feedback-topology designs for interference alignment in MIMO interference channels. *IEEE Trans. Sig. Process.* **60**(12), 6561–6575 (2012)
18. O. El Ayach, S.W. Peters, R.W. Heath Jr., The practical challenges of interference alignment. *IEEE Wirel. Commun.* **20**(01), 35–42 (2013)
19. N. Zhao, F. Richard Yu, M. Jin, Q. Yan, V.C.M. Leung, Interference Alignment and Its Applications: A Survey, Research Issues and Challenges. *IEEE Commun. Surv. Tutor.* **18**(3), 1779–1803 (2016)
20. Y. Fadlallah, K. Amis, A. Aissa-El-Bey, R. Pyndiah, Interference Alignment for a multi-user SISO interference channel. *EURASIP J. Wirel. Commun. Netw.* <https://doi.org/10.1186/1687-1499-2014-79>
21. Q. Sun, S. Han, Z. Xu, S. Wang, I. Chih-Lin, Z. Pan, in *IEEE wireless communications and networking conference (WCNC)*. Sum rate optimization for MIMO non-orthogonal multiple access systems (IEEE, Istanbul, 2015), pp. 747–752
22. Z. Ding, R. Schober, H.V. Poor, A general MIMO framework for NOMA downlink and uplink transmission based on signal alignment. *IEEE Trans. Wirel. Commun.* **15**(06), 4438–4454 (2016)
23. Y. Liu, G. Pan, H. Zhang, M. Song, On the capacity comparison between MIMO-NOMA and MIMO-OMA. *IEEE Access.* **04**, 2123–2129 (2016)
24. Z.Q. Al-Abbasi, D.K.C. So, J. Tang, in *IEEE international communications conference (ICC)- wireless communications symposium*. Resource Allocation for MU-MIMO non-orthogonal multiple access (NOMA) system with interference alignment (IEEE, Paris, 2017), pp. 1–6
25. H. Sung, S.H. Park, K.J. Lee, I. Lee, Linear precoder designs for K user interference channels. *IEEE Trans. Wirel. Commun.* **9**(01), 291–301 (2010)
26. I. Santamaria, O. Gonzalez, R. Heath, S. Peters, in *IEEE GLOBECOM*. Maximum sum rate interference alignment algorithms for MIMO channels (IEEE, Miami, 2010), pp. 1–6
27. T.E. Brudan, J. Eiksson, V. Koivunen, Steepest descent algorithms for optimization under unitary matrix constraint. *IEEE Trans. Sig. Process.* **56**(03), 1134–1147 (2006)
28. Y. Nishimori, S. Akaho, S. Abdallah, M. Plumbley, in *IEEE conference on acoustics, speech, and signal processing*. Flag Manifolds for Subspace ICA Problems (IEEE, Honolulu-HI-USA, 2017)
29. A. Edelman, T.A. Arias, S.T. Smith, The Geometry of algorithms with orthogonality constraints. *SIAM J. Matrix Anal. Appl.* **20**(2), 303–353 (1998)
30. S. Ye, R.S. Blum, Optimized signaling for MIMO interference systems with feedback. *IEEE Trans. Sig. Process.* **51**(11), 2839–2848 (2003)
31. M.S. Ali, E. Hossain, D.J. Kim, Non-orthogonal multiple access (NOMA) for downlink multiuser MIMO systems: User clustering, beamforming, and power allocation. *IEEE Access J. Phys. Mediu. Access Control. Layer Adv. 5G Wirel. Netw.* **05**, 565–577 (2016)
32. M.S. Ali, H. Tabassum, E. Hossain, Dynamic user clustering and power allocation in non-orthogonal multiple access (NOMA) systems. *IEEE Access.* **04**, 6325–6343 (2016)

Submit your manuscript to a SpringerOpen[®] journal and benefit from:

- Convenient online submission
- Rigorous peer review
- Open access: articles freely available online
- High visibility within the field
- Retaining the copyright to your article

Submit your next manuscript at ► [springeropen.com](https://www.springeropen.com)
